Thieme

Increased Glycolytic Activity Is Part of Impeded M1(LPS) Macrophage Polarization in the Presence of Urolithin A#

Authors
Sheyda Bahiraii[1,2], Barbara Braunböck-Müller[1], Elke H. Heiss[1]

Affiliations
1 Department of Pharmaceutical Sciences/Pharmacognosy, University of Vienna, Vienna, Austria
2 Vienna Doctoral School of Pharmaceutical, Nutritional and Sport Sciences, University of Vienna, Vienna, Austria

Key words
urolithin A, anti-inflammatory, macrophages, M1 polarization, glycolysis

received September 13, 2023
accepted after revision November 9, 2023

Bibliography
Planta Med 2024; 90: 546–553
DOI 10.1055/a-2240-7462
ISSN 0032-0943

Georg Thieme Verlag KG, Rüdigerstraße 14,
70469 Stuttgart, Germany

Correspondence
Assoc. Prof. Dr. Elke H. Heiss
Department of Pharmaceutical Sciences/Pharmacognosy,
Cellular Stress Resistance Team, University of Vienna
Josef Holaubek Platz 2 (UZA2), 1090 Vienna, Austria
Phone: +43 1 4 27 75 59 93, Fax: +43 1 42 77 95 52
elke.heiss@univie.ac.at

Supplementary material is available under https://doi.org/10.1055/a-2240-7462

ABSTRACT

Urolithin A is a gut metabolite of ellagitannins and reported to confer health benefits, e.g., by increased clearance of damaged mitochondria by macroautophagy or curbed inflammation. One targeted cell type are macrophages, which are plastic and able to adopt pro- or anti-inflammatory polarization states, usually assigned as M1 and M2 macrophages, respectively. This flexibility is tightly coupled to characteristic shifts in metabolism, such as increased glycolysis in M1 macrophages, and protein expression upon appropriate stimulation. This study aimed at investigating whether the anti-inflammatory properties of **u**rolithin A may be driven by metabolic alterations in cultivated murine M1(lipopolysaccharide) macrophages. Expression and extracellular flux analyses showed that urolithin A led to reduced *il1β, il6*, and *nos2* expression and boosted glycolytic activity in M1(lipopolysaccharide) macrophages. The pro-glycolytic feature of **urolithin A** occurred in order to causally contribute to its anti-inflammatory potential, based on experiments in cells with impeded glycolysis. Mdivi, an inhibitor of mitochondrial fission, blunted increased glycolytic activity and reduced M1 marker expression in M1(lipopolysaccharide/**urolithin A**), indicating that segregation of mitochondria was a prerequisite for both actions of **urolithin A**. Overall, we uncovered a so far unappreciated metabolic facet within the anti-inflammatory activity of **urolithin A** and call for caution about the simplified notion of increased aerobic glycolysis as an inevitably proinflammatory feature in macrophages upon exposure to natural products.

Introduction

Urolithin A (UroA) is one metabolite of ellagitannins produced by intestinal microbes and proposed to be one of the active bioavailable principles of ellagitannins taken up with fruits, berries, or nuts as part of a diet or herbal preparation. It is favorably produced by a microbiome characterized by a higher Firmicutes to Bacteroidetes ratio and a greater abundance of *Clostridiales, Ruminococcaceae*, and *Akkermansia muciniphilia* [1]. Multiple strains possess the ability to metabolize ellagic acids to UroA, including *Bifidobacterium pseudocatenulatum* INIA P815, *Enterococcus faecium* FUA027, and *Lactococcus garvieae* FUA009 (isolated from fecal samples) as well as *Streptococcus thermophilus* FUA329 (isolated

Dedicated to Professors Rudolf Bauer, Chlodwig Franz, Brigitte Kopp, and Hermann Stuppner for their invaluable contributions and commitment to Austrian Pharmacognosy.

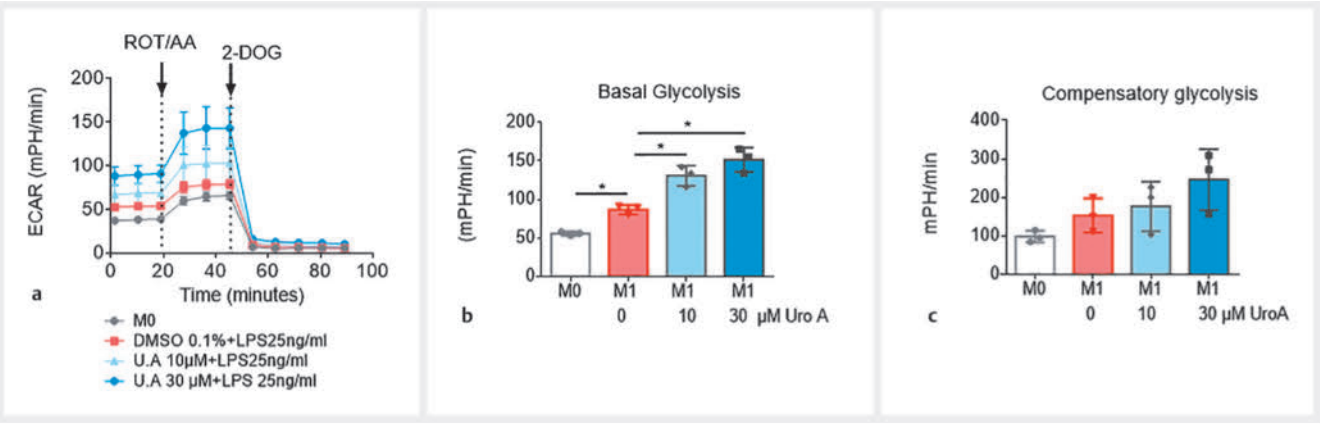

▶ **Fig. 1** M1(LPS/UroA) display higher glycolytic activity than M1(LPS) macrophages. IBMDM macrophages were pretreated with DMSO or with the indicated concentrations of UroA for 30 min before they were stimulated with LPS (25 ng/mL) for 16 h. Then, 100 000 cells were subjected to a glycolytic rate assay and extracellular flux analysis as described in detail in the Methods section. Panel **a** depicts an overview of glycolytic activity over time before and after the addition of the OXPHOS inhibitors rotenone (ROT) and antimycin A (A.A) (= driving cells from basal to compensatory glycolytic activity) or the glycolysis inhibitor DOG (= showing glycolysis-independent acidification), as evident in the extracellular acidification rate (ECAR) in mPH/min. **b** Basal glycolytic activity. **c** Compensatory glycolytic activity. Bar graphs derive from compiled data of three different biological replicates given as the mean ± SD ($^*p < 0.05$; ANOVA, followed by multiple comparisons test).

from human milk) [2]. A recent study added *Enterocloster bolteae* CEBAS S4A9, *E. bolteae* DSM 29485, *E. bolteae* DSM 15670 T, *Enterocloster asparagiformis* DSM 15981 T, and *Enterocloster citroniae* DSM 19261 T to the UroA producers (all strains were isolated from fecal samples) [3]. UroA has been reported to confer several potential benefits, including a prolonged health span [4], improved muscle function [5], or reduced inflammation. Concerning inflammation, UroA has been heavily investigated in the context of colitis, where it could protect gut barrier function or improve dysbiosis [6–8]. *In vitro*, UroA has been shown to reduce proinflammatory signaling in macrophages, osteoclasts, neutrophils, and T cells [9–11]. Reported molecular modes of action of UroA include binding to cytochrome P450 (Cyp) 1A1, activation of the aryl hydrocarbon receptor (AhR) or nuclear factor E2-related factor 2 (Nrf2), and inhibition of nuclear factor (NF)-κB or mechanistic target of rapamycin (mTOR) signaling; the latter is closely linked to induction of macroautophagy, in particular mitophagy, which is considered one prime mechanism underlying the bioactivities of UroA [12–15].

Macrophages are part of the innate immune system and have a variety of functions, comprising control of infection and inflammation, phagocytic clearance of debris, or building a bridge to the adaptive immune system by antigen processing and presentation to T cells [16]. The distinct tasks demand that macrophages are highly plastic and can adopt distinctive functional phenotypes (polarization states). They originally were divided into classically activated proinflammatory M1 and the alternatively activated anti-inflammatory M2 type, which represent only the extremes of a continuum of possible distinct intermediates. Proinflammatory macrophages are typically induced by interferon (IFN)-γ [referred to as M1(IFN)-γ, lipopolysaccharide (LPS) [M1(LPS)] or a combination of both [M1(IFN/LPS)] and express typical M1 markers, such as interleukin (IL)1β, IL6, tumor necrosis factor (TNF)-α, or inducible nitric oxide (NO) synthase (NOS2). M2(a) macrophages develop after stimulation with IL 4 [M2(IL4)] or 13 [M2(IL13)] and are involved in tissue remodeling and wound repair, and express IL10, transforming growth factor (TGF)-β arginase 1, mannose receptor (Mrc1; CD206), or C-type lectines (Mgl1/2) [17]. Notably, macrophage polarization coincides and is partly dependent on characteristic shifts in cellular energy metabolism for optimal supply with ATP, electrons, building blocks, and substrates for posttranslational modifications (immunometabolism). Murine M1 macrophages usually show elevated activity of aerobic glycolysis, a broken tricarboxylic acid (TCA) cycle, as well as use of mitochondria for reactive oxygen species (ROS) rather than for ATP production. M2 macrophages, in contrast, tend to run coupled oxidative phosphorylation (OXPHOS) with augmented fatty acid oxidation, an intact TCA cycle, or an increased hexosamine pathway [18].

This study set out to investigate a potential immunometabolic facet of UroA, i.e., to address the question whether modulated bioenergetic programs in response to UroA exposure may directly account for altered M1(LPS) macrophage polarization *in vitro*.

Results and Discussion

We first investigated macrophage polarization from naïve M0 to M1(LPS) or M2(IL4) in the absence and presence of UroA. A resazurin conversion assay showed that concentrations up to 30 µM of UroA were safe for macrophage viability (**Fig. 1SA**, Supporting Information), whereas staurosporine, a known proapoptotic compound [19], strongly diminished cell vitality. Typical M1 marker expression based on *il1β, il6,* and *nos2* mRNA expression as well as NO and TNF-α release were reduced by 10 and 30 µM UroA in M1(LPS) macrophages, again in line with published reports [20, 21] (**Fig. 1SB-F**, Supporting Information). Sulforaphane was used as a reference compound due to its reported inhibition of M1 (LPS) polarization [22]. IL4-triggered induction of *arg1, mrc1,*

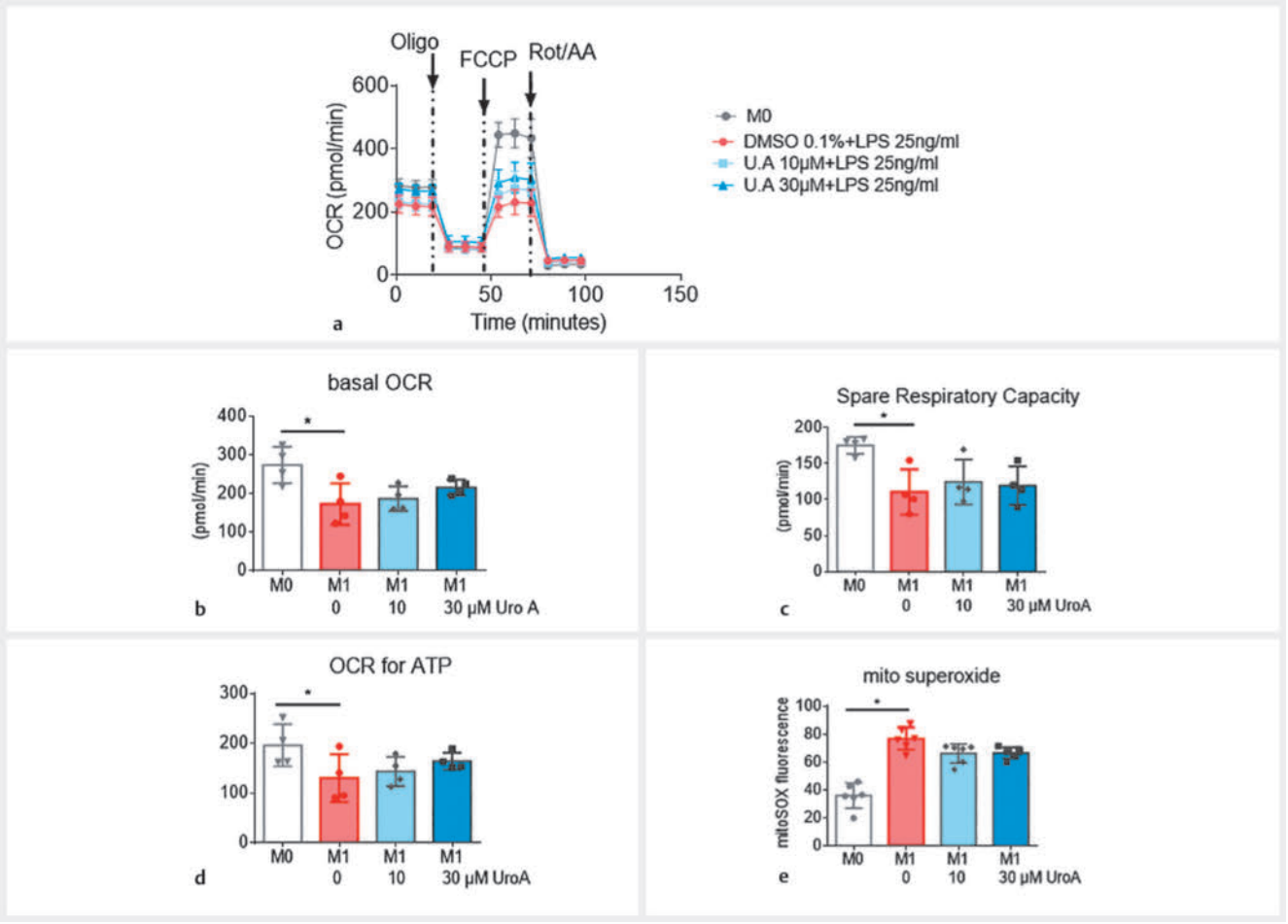

▶ **Fig. 2** Both M1(LPS) and M1(LPS/UroA) show impaired OXPHOS activity and higher mitochondrial superoxide production than M0 macrophages. IBMDM macrophages were pretreated with DMSO or with the indicated concentrations of UroA for 30 min before they were stimulated with LPS (25 ng/mL) for 16 h. Then, 100 000 cells were subjected to a mitochondrial stress test and extracellular flux analysis as described in detail in the Methods section. Panel **a** depicts OXPHOS activity, as evident in the oxygen consumption rate (OCR) in pmol/min, over time before and after the addition of the ATP synthase inhibitor oligomycin (oligo) (= allowing deduction of OCR coupled to ATP production), the uncoupler FCCP (= eliciting maximal OCR), and the complex I/III inhibitors rotenone (rot) and antimycin A (A.A) (= showing non-mitochondrial OCR). **b** Basal respiration, **c** spare respiratory capacity, and **d** OCR coupled to ATP synthesis. **e** Mitochondrial superoxide generation was measured by MitoSOX staining and the fluorescent signal was quantified by flow cytometry. Bar graphs derive from compiled data of three different biological replicates given as the mean ± SD (*$p < 0.05$; ANOVA, followed by multiple comparisons test).

mgl1, and *2* mRNA and polyamine or TGF-*β* release were not markedly affected by the presence of UroA (**Fig. 2SA-E**, Supporting Information), although UroA was reported to elicit a modest increase in M2 marker expression when macrophages were exposed to both IL4 and IL13 [23]. Overall, this data partly confirms previous findings or shows that UroA can impede M1(LPS), but not M2(IL4) polarization in macrophages (prevention setting). A potential influence on M1 → M2 or M2 → M1 repolarization (potential therapy setting) was beyond the scope of this study, but clearly deserves further investigation in the future.

Given that macrophage polarization is driven by distinct metabolic programs, we next examined the influence of UroA on glycolytic (needed for M1 polarization) and respiratory activity (favored during M2 polarization). As expected from previous reports [24] in cultured murine macrophages, M1(LPS) cells showed higher glycolytic activity than M0, as evident in an extracellular flux assay using the Seahorse technology. Despite the observed anti-inflammatory action of UroA in macrophages and the presumably proinflammatory characteristic of glycolysis, the presence of UroA further enhanced basal and tendentially also compensatory glycolytic activity in M1(LPS) cells (▶ **Fig. 1**). Looking at mitochondrial metabolism, UroA could not prevent the drop of respiratory activity assessed as oxygen consumption rates (OCR) in M1(LPS) cells, at least at the investigated time point and UroA concentrations, although UroA has already been reported to protect mitochondrial function [23]. Basal, spare, and coupled respiration were not significantly different to control M1(LPS). UroA did not prevent either the mitochondrial superoxide production during M1(LPS) polarization (▶ **Fig. 2**), presumed to occur due to breaks in the TCA cycle, succinate accumulation, and reverse electron transport at complex I in the mitochondrial membrane [25].

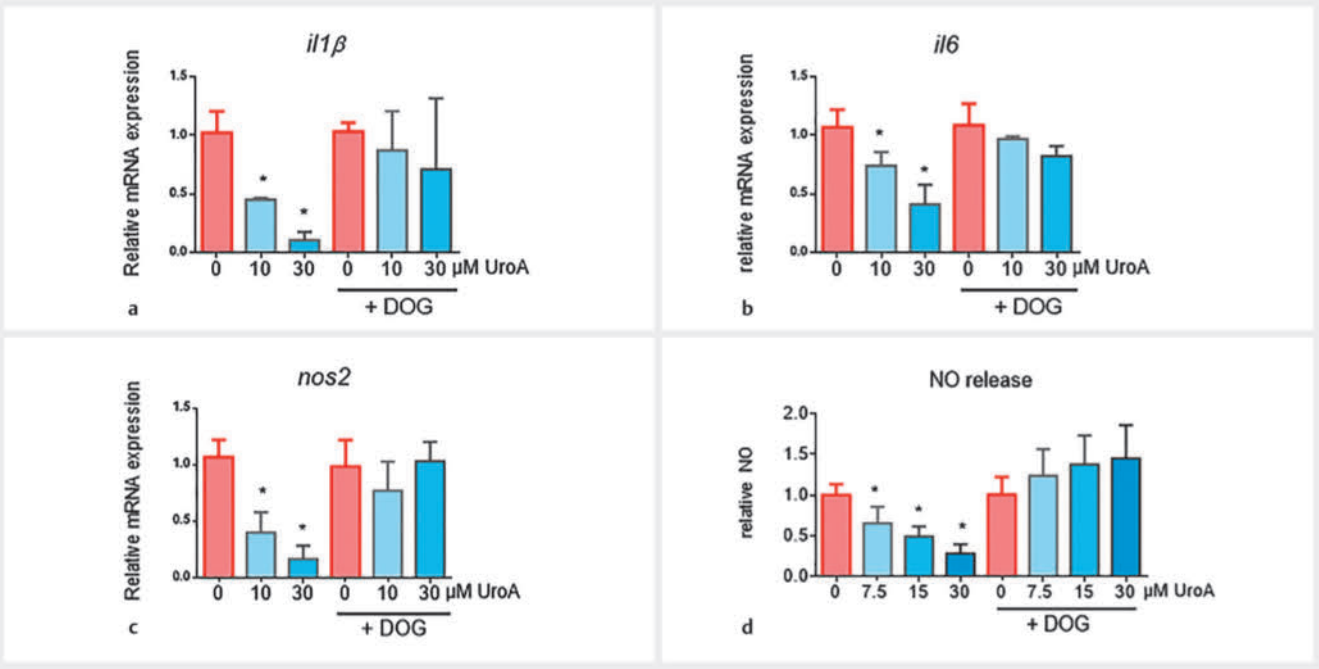

▶ **Fig. 3** Interference with glycolytic activity blunts the inhibition of M1(LPS) marker expression by UroA. iBMDMs were left untreated or treated with DOG (2 mM) and exposed to Uro A (10 and 30 µM) as indicated for 30 min prior to stimulation with LPS (25 ng/mL) for 6 h. Then, mRNA expression [relative to the respective M1(LPS) control w/o UroA] was assessed for (**a**) *il1β*, (**b**) *il6*, and (**c**) *nos 2* by qPCR (using *ppia* as the reference gene). **d** Cells were left untreated or treated with DOG (2 mM) and exposed to Uro A (0–30 µM) as indicated for 30 min prior to stimulation with LPS (25 ng/mL) for 24 h. Then, NO release was quantified by the Griess assay and referred to the respective M1(LPS) control without UroA treatment. Bar graphs depict compiled data from three biological replicates (mean ± SD, n = 3, $^*p < 0.05$, ANOVA, compared to respective solvent control).

Next, we were prompted to examine whether the observed increased glycolytic activity may be implicated in the blunted M1 (LPS) polarization by UroA, especially as the simplistic view of elevated glycolysis as an essential M1 prerequisite and invariably proinflammatory feature had already been questioned [22, 26, 27]. For this, the inhibitory effect of UroA on M1 marker expression (*il1β, il6*, and *nos2* mRNA as well as NO release) was compared under normal and conditions of partially inhibited glycolysis. Diminishing glycolytic activity by the pharmacological inhibitor deoxyglucose (DOG) at a concentration of 2 mM (which achieved submaximal inhibition but still allowed moderate M1 marker gene expression as confirmed in our previous study [22]) dampened the relative inhibitory activity of UroA towards all selected readouts (▶ **Fig. 3**). Therefore, the observed increased glycolytic activity may truly take part in the UroA-mediated inhibition of M1(LPS) polarization. The increased glycolytic activity was not associated with an elevated expression of enzymes, characteristic for proinflammatory macrophages like hexokinase 2, pyruvate kinase M2, or lactate dehydrogenase on mRNA (**Fig. 3S**, Supporting Information) or protein (not shown) level. However, this does not yet allow a reliable deduction about possibly altered enzymatic activities due to posttranslational or allosteric modification, which would require further examination. Notably, M1(LPS/UroA) did not take up more glucose than M1(LPS) either (**Fig. 3S**, Supporting Information), suggesting that M1(LPS/Uro) preferentially fuels the incorporated glucose into aerobic glycolysis rather than into mitochondrial respiration.

The question of how to reconcile the observed elevated glycolysis and impaired mitochondrial OXPHOS with the generally accepted pro-mitophagic, mitoprotective, and herewith connected anti-inflammatory activity of UroA still remains [28–30]. The process of mitophagy involves mitochondrial fission, i.e., the segregation of one big mitochondrium into smaller ones, engulfment by phagosomes, and temporary higher glycolytic activity to replenish ATP during the phase of reduced mitochondrial ATP production [31]. Thus, it may be conceivable that UroA – in the context of its pro-mitophagic activity – leads to (transient) mitochondrial fission in macrophages, which entails reduced respiration and increased glycolysis. Using a mitochondria-selective dye and confocal microscopy, M1(LPS/UroA) macrophages indeed showed transient fission of mitochondria, which occurred much earlier (8 h) than in control M1(LPS) (at 24 h; as part of their full polarization to M1 cells [32] (▶ **Fig. 4**). To see whether this early fission accounts for glycolytic and anti-inflammatory activity of UroA, we made use of mdivi, an accepted inhibitor of mitochondrial fission [33, 34]. The presence of mdivi blunted LPS-triggered induction of investigated M1 markers (based on published reports [35, 36]) but also diminished the extent of UroA-mediated inhibition of their expression (▶ **Fig. 5a**, from approx. 80–100% down to ~ 20–30% inhibition only). Moreover, mdivi overcame the increased glycolytic activity in M1(LPS/UroA) when compared to M1(LPS) macrophages (▶ **Fig. 5b**).

Overall, this study shows that UroA reduces the expression of proinflammatory genes and elicits higher glycolytic activity in M1

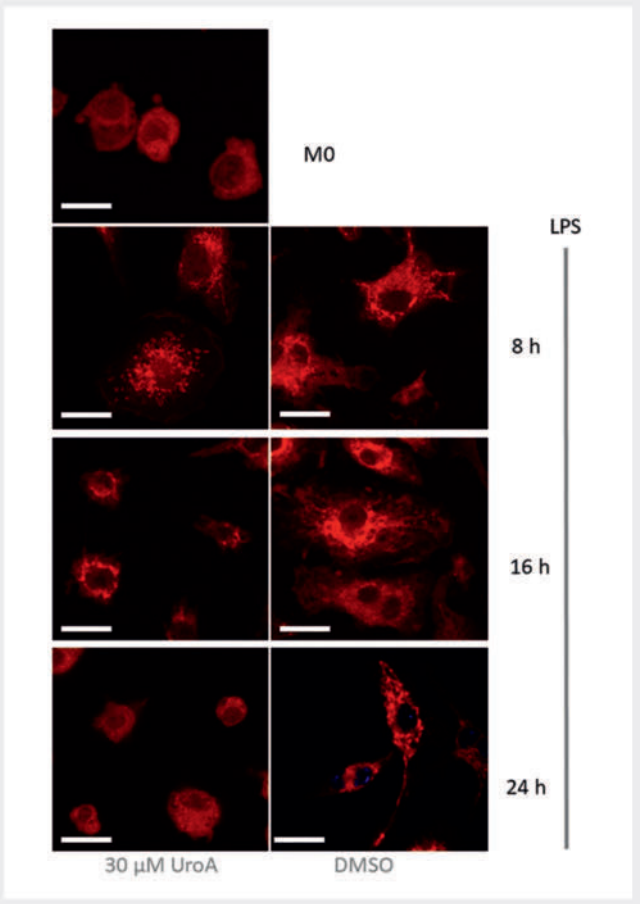

▶ **Fig. 4** UroA leads to comparably early and transient mitochondrial fission in M1(LPS) macrophages. iBMDMs were left as is (M0) or treated with vehicle (0.1% DMSO) or UroA (30 µM) for 30 min prior to stimulation with LPS (25 ng/mL) for the indicated periods of time. A MitoTracker Deep Red probe was used to detect changes in mitochondrial morphology by maximum intensity projection (MIP) imaged by confocal microscopy. The scale bar indicates 10 µm. Representative images are shown.

(LPS) macrophages. The increased glycolytic activity is needed for maximal inhibitory action of UroA and might be explained as a compensatory response to mitochondrial fission, occurring as a prerequisite for boosted mitophagy by UroA. These findings disclose a so far unappreciated facet in the anti-inflammatory activity of UroA and support the notion that increased glycolytic does not always need to result in a proinflammatory outcome but can also contribute to anti-inflammatory signal relays. What still remains to be resolved in more detail, though, is whether the increased glycolytic activity is only required for proper mitophagy, which then mediates the anti-inflammatory action in UroA-treated cells [30], or whether it also directly modulates inflammatory signaling, e.g., by providing metabolites as precursors for epigenetic posttranslational modifications or lactate as an anti-inflammatory metabolite and signal [37, 38]. Moreover, it needs to be noted that experiments were performed in cultivated murine macrophages with LPS as the sole trigger for M1 polarization and on only few selected time points. Therefore, further studies are needed, as, e.g., possibly altered behavior of M1(IFN/LPS) or M1 (IFN) macrophages, fuel competition and crosstalk between different (immune) cells, dynamic cellular responses during inflammation, or differences between human and murine macrophage biology were not considered [39–43]. In addition, for application of UroA in an *in vivo* setting, one should keep in mind that its metabolization to (less active) phase II metabolites, such as glucuronides or sulfates, may hamper bioactivity [9], and that *in vivo* achievable levels of UroA may well be below 10 or 30 µM, however, with likely local peaks in the colon or sites of inflammation [44, 45].

Materials and Methods

Reagents, chemicals, and cells

Stimuli for macrophage polarization, i.e., LPS from *Escherichia coli O55:B5* and mouse IL4, as well as 2-deoxy-D-glucose (2-DOG), sodium pyruvate, α-D-glucose, sulfanilamide, naphthylendiamine, and mdivi were obtained from Sigma-Aldrich. UroA came from Tocris. DMSO served as the vehicle control and solvent for all stock solutions and was obtained from Sigma. The DMSO concentration was even throughout the different conditions of one experiment and never exceeded a final concentration of 0.2%. Media and supplements for cell culture were purchased from Invitrogen, Lonza, or Sigma. Immortalized bone marrow-derived macrophages (iBMDMs) were kindly provided by Laszlo Nagy (Debrecen University, Hungary) and the RAW 264.7 cell line came from ATCC.

Cultivation and treatment of murine macrophages

The detailed protocol was previously published in [22]. Briefly, iBMDMs were cultured in phenol red-free DMEM high glucose supplemented with 10% filtered L-929 cell-conditioned medium containing macrophage colony-stimulating factor (M-CSF), 10% heat-inactivated FBS, 2 mM L-glutamine, 100 IU/mL penicillin, and 100 mg/mL streptomycin (iBMDM medium) at 37 °C with 5% CO_2. RAW 264.7 were cultivated in DMEM high glucose supplemented with 10% heat-inactivated FBS, 2 mM L-glutamine, 100 IU/mL penicillin, and 100 mg/mL streptomycin. Cells were seeded into appropriate plates and left overnight prior to polarization and treatment as indicated. Both cell lines gave consistent results in the assessed readouts.

Assessment of nitric oxide/nitrite

Cells in 96-well plates (3×10^4 cells per well in 200 µL) were treated as indicated. Then, an aliquot (100 µL) of the cell culture supernatant was mixed with an even volume of Griess reagent (0.5% sulfanilamide, 0.05% naphthylendiamine) before absorbance at 550 nm was assessed using a microplate spectrophotometer (TECAN Sunrise Austria).

Ribonucleic acid extraction and real time quantitative polymerase chain reaction analysis

The detailed protocol has already been published in [22]. Briefly, total ribonucleic acid (RNA) from 0.5–1 million cells was extracted using an RNA isolation kit (IST Innuscreen GmbH), quantified, and checked for purity using a NanoDrop 2000 (Thermo Fisher Scien-

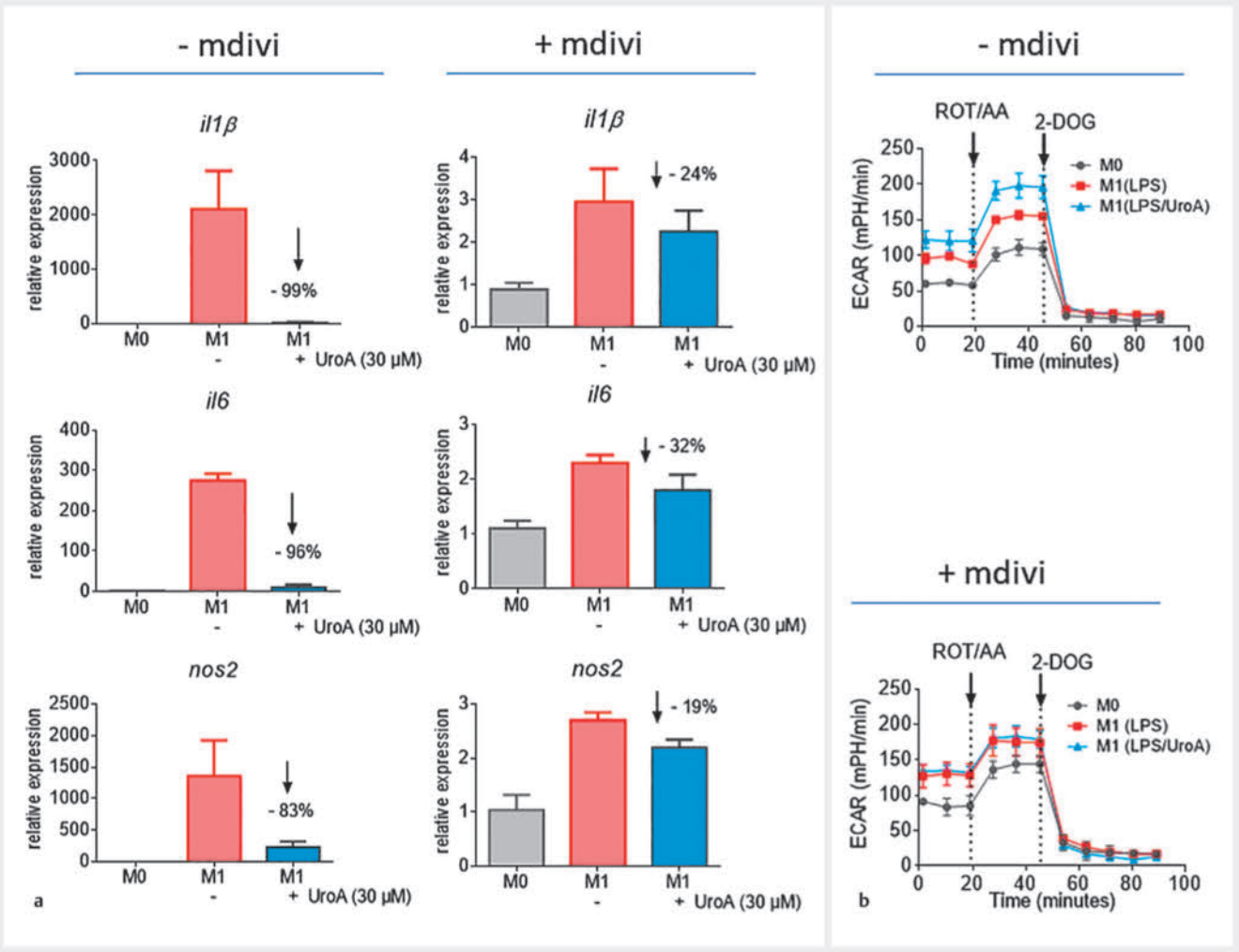

▶ **Fig. 5** Reduced M1 marker expression and boosted glycolytic activity in M1(LPS/UroA) is blunted by mdivi, an inhibitor of mitochondrial fission. **a** Murine macrophages (RAW 264.7) were pretreated with DMSO or UroA (30 µM) for 30 min before they were stimulated with LPS (25 ng/mL) in the presence and absence of mdivi (25 µM) for 16 h. Then, mRNA expression (relative to the respective M0 control w/o LPS) was assessed for (**a**) *il1β*, (**b**) *il6*, and (**c**) *nos 2* by qPCR (using *ppia* as the reference gene). **b** Murine macrophages (RAW 264.7) were pretreated with DMSO or UroA (30 µM) for 30 min before they were stimulated with LPS (25 ng/mL) in the presence and absence of mdivi (25 µM) for 16 h. Then, 100 000 cells were subjected to a glycolytic rate assay and extracellular flux analysis as described in detail in the Methods section. An overview of glycolytic activity over time before (= basal glycolytic activity) and after the addition of the OXPHOS inhibitors rotenone (ROT) and antimycin A (A.A) (= driving cells from basal to compensatory glycolytic activity) or the glycolysis inhibitor DOG (= showing glycolysis-independent acidification) is depicted. The graphs are representative for two biological replicates [in technical triplicate or quadruplicate in case of **b**] with consistent results.

▶ **Table 1** Primer sequences for qPCR experiments.

nos2	*Fwd : CAGAGGACCCAGAGACAAGC* *Rev : TGCTGAAACATTTCCTGTGC*
il6	*Fwd : GAGGATACCACTCCCAACAGACC* *Rev : AAGTGCATCATCGTTGTTCATACA*
il1β	*Fwd : CAACCAACAAGTGATATTCTCCATG* *Rev : GATCCACACTCTCCAGCTGCA*
ppia	*Fwd : CCAAGACTGAATGGCTGGATG* *Rev : TGTCCACAGTCGGAAATGGTG*

tific). cDNA was synthesized from 1 µg of RNA using a High-Capacity cDNA Reverse Transcription Kit (Thermo Fisher), and then subjected to quantitative polymerase chain reaction (qPCR) using the Luna Universal qPCR Master Mix (New England Biolab) and the LightCycler 480 Real-Time PCR System (Roche Diagnostics GmbH). Data analysis was performed using the ($2^{-\Delta\Delta Ct}$) method. Primer sequences are listed in ▶ **Table 1**.

Extracellular flux analysis (Seahorse technology)

The detailed procedure can be found in [22]. In short, cells were treated, scraped, and plated in XF24e-cell culture plates precoated with Corning Cell-Tak adhesive (Sigma-Aldrich) at a density of 1×10^5 cells/well. After 1 h at 37 °C in a non-CO_2 incubator in XF assay medium (pH 7.4/37 °C) (Agilent Technologies) supple-

mented with 2 mM glutamine, 1 mM pyruvate and 25 mM glucose real-time extracellular acidification (ECAR) and OCR rates were assessed in an XF24e Flux Analyzer (Seahorse Bioscience, now Agilent Technologies). ECAR and OCR were monitored under basal conditions, as well as after rotenone (Rot, 0.5 µM)/antimycin A (AA; 0.5 µM), FCCP (1 µM), and 2-DOG injections (50 mM), respectively, using the proprietary glycolytic rate assay and mitochondrial stress test protocols from Agilent. Data were analyzed using the Wave software package and report generators were provided by Agilent Technologies.

Assessment of mitochondrial superoxide

Cells were seeded on 12-well plates (5×10^5 cells per well) and treated as indicated. The following day, cells were washed with PBS and incubated with 5 µM MitoSOX (Thermo Fisher Scientific) in Hank's balanced salt solution with calcium and magnesium (HBSS/Ca/Mg) (Gibco) for 10 min at 37 °C. After washing with PBS, the red fluorescence intensity was detected and quantified by flow cytometry [FACSCalibur (BD Biosciences)].

Confocal imaging of mitochondrial morphology

Cells were seeded at a density of 5×10^5 per well in 12-well plates containing coverslips and treated as indicated. Then, they were washed with PBS and incubated with DMEM medium supplemented with 250 nM MitoTracker Deep Red FM (Invitrogen) for 20 min at 37 °C according to the manufacturer's instructions. The medium was removed, and cells were fixed with 4% MeOH-free paraformaldehyde for 10 min at 37 °C. Following the fixation step, cells were rinsed three times in PBS and mounted in Fluoromount Aqueous Mounting Medium (Sigma). MitoTracker Deep Red fluorescence with excitation/emission maxima of 644/665 nm was detected using a confocal microscope (Olympus), and images were collected and analyzed by Leica Application Suite X (LAS X) image analysis software.

Statistics

Unless stated otherwise, at least three independent biological replicates were performed per experiment. The bar graphs depict the mean ± SD (standard deviation). Groups were compared via ANOVA and multiple comparisons test by using GraphPad Prism 9 software. Differences were considered as significant if $p < 0.05$.

Supporting information

Experimental protocols and data regarding the influence of UroA on cell viability, expression of M1(LPS), M2(IL4) markers, or glycolytic enzymes as well as on cellular glucose uptake rates are available as Supporting Information.

Contributors' Statement

S. B. designed and performed the experiments, analyzed and interpreted data, prepared figures, and contributed to writing and finalizing the manuscript. B. B. performed and analyzed the experiments. E. H. H. conceived and supervised the study, provided funding, performed experiments, and drafted the manuscript. All authors have read and agreed to the submitted version of the manuscript.

Funding

This work was financed by the Austrian Science Fund FWF (P32600 to EHH).

Acknowledgements

The authors thank Prof. L. Nagy for kindly providing iBMDMs, D. Schacher and S. Hummelbrunner for excellent technical support, M. Peteri and R. Guimarães Machado Vaz da Silva for their hands-on help during their internships as well as the entire Molecular Targets Group at Pharmacognosy/UniVie for fruitful input and discussions.

Conflict of Interest

The authors declare that they have no conflict of interest.

References

[1] Tomás-Barberán FA, González-Sarrías A, García-Villalba R, Núñez-Sánchez MA, Selma MV, García-Conesa MT, Espín JC. Urolithins, the rescue of "old" metabolites to understand a "new" concept: Metabotypes as a nexus among phenolic metabolism, microbiota dysbiosis, and host health status. Mol Nutr Food Res 2017; 61: 1500901

[2] Xia M, Mu S, Fang Y, Zhang X, Yang G, Hou X, He F, Zhao Y, Huang Y, Zhang W, Shen J, Liu S. Genetic and probiotic characteristics of urolithin a producing *Enterococcus faecium* FUA027. Foods 2023; 12: 1021

[3] Iglesias-Aguirre CE, García-Villalba R, Beltrán D, Frutos-Lisón MD, Espín JC, Tomás-Barberán FA, Selma MV. Gut bacteria involved in ellagic acid metabolism to yield human urolithin metabotypes revealed. J Agric Food Chem 2023; 71: 4029–4035

[4] D'Amico D, Andreux PA, Valdés P, Singh A, Rinsch C, Auwerx J. Impact of the natural compound urolithin a on health, disease, and aging. Trends Mol Med 2021; 27: 687–699

[5] Luan P, D'Amico D, Andreux PA, Laurila PP, Wohlwend M, Li H, Imamura de Lima T, Place N, Rinsch C, Zanou N, Auwerx J. Urolithin A improves muscle function by inducing mitophagy in muscular dystrophy. Sci Transl Med 2021; 13: eabb0319

[6] Ma M, Wang Y, Fan S, Huang Y, Su X, Lu C. Urolithin A alleviates colitis in mice by improving gut microbiota dysbiosis, modulating microbial tryptophan metabolism, and triggering AhR activation. J Agric Food Chem 2023; 71: 7710–7722

[7] Ghosh S, Moorthy B, Haribabu B, Jala VR. Cytochrome P450 1A1 is essential for the microbial metabolite, Urolithin A-mediated protection against colitis. Front Immunol 2022; 13: 1004603

[8] Singh R, Chandrashekharappa S, Bodduluri SR, Baby BV, Hegde B, Kotla NG, Hiwale AA, Saiyed T, Patel P, Vijay-Kumar M, Langille MGI, Douglas GM, Cheng X, Rouchka EC, Waigel SJ, Dryden GW, Alatassi H, Zhang HG, Haribabu B, Vemula PK, Jala VR. Enhancement of the gut barrier integrity by a microbial metabolite through the Nrf2 pathway. Nat Commun 2019; 10: 89

[9] Bobowska A, Granica S, Filipek A, Melzig MF, Moeslinger T, Zentek J, Kruk A, Piwowarski JP. Comparative studies of urolithins and their phase II metabolites on macrophage and neutrophil functions. Eur J Nutr 2021; 60: 1957–1972

[10] Mei M, Lei Y, Ouyang L, Zhao M, Lu Q. Deficiency of Pink1 promotes the differentiation of Th1 cells. Mol Immunol 2023; 160: 23–31

[11] Tao H, Li W, Zhang W, Yang C, Zhang C, Liang X, Yin J, Bai J, Ge G, Zhang H, Yang X, Li H, Xu Y, Hao Y, Liu Y, Geng D. Urolithin A suppresses RANKL-induced osteoclastogenesis and postmenopausal osteoporosis by, suppresses inflammation and downstream NF-κB activated pyroptosis pathways. Pharmacol Res 2021; 174: 105967

[12] Shen PX, Li X, Deng SY, Zhao L, Zhang YY, Deng X, Han B, Yu J, Li Y, Wang ZZ, Zhang Y. Urolithin A ameliorates experimental autoimmune encephalomyelitis by targeting aryl hydrocarbon receptor. EBioMedicine 2021; 64: 103227

[13] Dong F, Murray IA, Annalora A, Coslo DM, Desai D, Gowda K, Yang J, Wang D, Koo I, Hao F, Amin SG, Patterson AD, Marcus C, Perdew GH. Complex chemical signals dictate Ah receptor activation through the gut–lung axis. FASEB J 2023; 37: e23010

[14] Abdelazeem KNM, Kalo MZ, Beer-Hammer S, Lang F. The gut microbiota metabolite urolithin A inhibits NF-κB activation in LPS stimulated BMDMs. Sci Rep 2021; 11: 7117

[15] Pattingre S, Espert L, Biard-Piechaczyk M, Codogno P. Regulation of macroautophagy by mTOR and Beclin 1 complexes. Biochimie 2008; 90: 313–323

[16] Mills CD, Thomas AC, Lenz LL, Munder M. Macrophage: SHIP of Immunity. Front Immunol 2014; 5: 620

[17] Rőszer T. Understanding the mysterious M2 macrophage through activation markers and effector mechanisms. Mediators Inflamm 2015; 2015: 816460

[18] Jha AK, Huang SC, Sergushichev A, Lampropoulou V, Ivanova Y, Loginicheva E, Chmielewski K, Stewart KM, Ashall J, Everts B, Pearce EJ, Driggers EM, Artyomov MN. Network integration of parallel metabolic and transcriptional data reveals metabolic modules that regulate macrophage polarization. Immunity 2015; 42: 419–430

[19] Belmokhtar CA, Hillion J, Ségal-Bendirdjian E. Staurosporine induces apoptosis through both caspase-dependent and caspase-independent mechanisms. Oncogene 2001; 20: 3354–3362

[20] Rønning SB, Voldvik V, Bergum SK, Aaby K, Borge GIA. Ellagic acid and urolithin A modulate the immune response in LPS-stimulated U937 monocytic cells and THP-1 differentiated macrophages. Food Funct 2020; 11: 7946–7959

[21] Piwowarski JP, Kiss AK, Granica S, Moeslinger T. Urolithins, gut microbiota-derived metabolites of ellagitannins, inhibit LPS-induced inflammation in RAW 264.7 murine macrophages. Mol Nutr Food Res 2015; 59: 2168–2177

[22] Bahiraii S, Brenner M, Yan F, Weckwerth W, Heiss EH. Sulforaphane diminishes moonlighting of pyruvate kinase M2 and interleukin 1β expression in M1 (LPS) macrophages. Front Immunol 2022; 13: 935692

[23] Toney AM, Fan R, Xian Y, Chaidez V, Ramer-Tait AE, Chung S. Urolithin A, a Gut Metabolite, Improves Insulin Sensitivity Through Augmentation of Mitochondrial Function and Biogenesis. Obesity (Silver Spring) 2019; 27: 612–620

[24] Van den Bossche J, O'Neill LA, Menon D. Macrophage immunometabolism: Where are we (going)? Trends Immunol 2017; 38: 395–406

[25] Mills EL, Kelly B, Logan A, Costa ASH, Varma M, Bryant CE, Tourlomousis P, Däbritz JHM, Gottlieb E, Latorre I, Corr SC, McManus G, Ryan D, Jacobs HT, Szibor M, Xavier RJ, Braun T, Frezza C, Murphy MP, O'Neill LA. Succinate dehydrogenase supports metabolic repurposing of mitochondria to drive inflammatory macrophages. Cell 2016; 167: 457–470.e13

[26] Bae S, Park PSU, Lee Y, Mun SH, Giannopoulou E, Fujii T, Lee KP, Violante SN, Cross JR, Park-Min KH. MYC-mediated early glycolysis negatively regulates proinflammatory responses by controlling IRF4 in inflammatory macrophages. Cell Rep 2021; 35: 109264

[27] Vijayan V, Pradhan P, Braud L, Fuchs HR, Gueler F, Motterlini R, Foresti R, Immenschuh S. Human and murine macrophages exhibit differential metabolic responses to lipopolysaccharide – A divergent role for glycolysis. Redox Biol 2019; 22: 101147

[28] D'Amico D, Olmer M, Fouassier AM, Valdés P, Andreux PA, Rinsch C, Lotz M. Urolithin A improves mitochondrial health, reduces cartilage degeneration, and alleviates pain in osteoarthritis. Aging Cell 2022; 21: e13662

[29] Boakye YD, Groyer L, Heiss EH. An increased autophagic flux contributes to the anti-inflammatory potential of urolithin A in macrophages. Biochim Biophys Acta Gen Subj 2018; 1862: 61–70

[30] Jiang K, Li J, Jiang L, Li H, Lei L. PINK1-mediated mitophagy reduced inflammatory responses to *Porphyromonas gingivalis* in macrophages. Oral Dis 2023; 29: 3665–3676

[31] Ni HM, Williams JA, Ding WX. Mitochondrial dynamics and mitochondrial quality control. Redox Biol 2015; 4: 6–13

[32] Kapetanovic R, Afroz SF, Ramnath D, Lawrence GM, Okada T, Curson JE, de Bruin J, Fairlie DP, Schroder K, St John JC, Blumenthal A, Sweet MJ. Lipopolysaccharide promotes Drp1-dependent mitochondrial fission and associated inflammatory responses in macrophages. Immunol Cell Biol 2020; 98: 528–539

[33] Li YH, Xu F, Thome R, Guo MF, Sun ML, Song GB, Li RL, Chai Z, Ciric B, Rostami AM, Curtis M, Ma CG, Zhang GX. Mdivi-1, a mitochondrial fission inhibitor, modulates T helper cells and suppresses the development of experimental autoimmune encephalomyelitis. J Neuroinflammation 2019; 16: 149

[34] Deng Y, Li S, Chen Z, Wang W, Geng B, Cai J. Mdivi-1, a mitochondrial fission inhibitor, reduces angiotensin-II-induced hypertension by mediating VSMC phenotypic switch. Biomed Pharmacother 2021; 140: 111689

[35] Su ZZ, Li CQ, Wang HW, Zheng MM, Chen QW. Inhibition of DRP1-dependent mitochondrial fission by Mdivi-1 alleviates atherosclerosis through the modulation of M1 polarization. J Transl Med 2023; 21: 427

[36] Liu X, Zhang X, Niu X, Zhang P, Wang Q, Xue X, Song G, Yu J, Xi G, Song L, Li Y, Ma C. Mdivi-1 Modulates Macrophage/Microglial Polarization in Mice with EAE via the Inhibition of the TLR2/4-GSK3β-NF-κB Inflammatory Signaling Axis. Mol Neurobiol 2022; 59: 1–16

[37] Diskin C, Ryan TAJ, O'Neill LAJ. Modification of proteins by metabolites in immunity. Immunity 2021; 54: 19–31

[38] Wu D, Zhang K, Khan FA, Wu Q, Pandupuspitasari NS, Tang Y, Guan K, Sun F, Huang C. The emerging era of lactate: A rising star in cellular signaling and its regulatory mechanisms. J Cell Biochem 2023; 124: 1067–1081

[39] Kedia-Mehta N, Finlay DK. Competition for nutrients and its role in controlling immune responses. Nat Commun 2019; 10: 2123

[40] Arner EN, Rathmell JC. Metabolic programming and immune suppression in the tumor microenvironment. Cancer Cell 2023; 41: 421–433

[41] Nikaein N, Tuerxun K, Cedersund G, Eklund D, Kruse R, Särndahl E, Nånberg E, Thonig A, Repsilber D, Persson A, Nyman E. Mathematical models disentangle the role of IL-10 feedbacks in human monocytes upon proinflammatory activation. J Biol Chem 2023; 299: 105205

[42] Cicchese JM, Evans S, Hult C, Joslyn LR, Wessler T, Millar JA, Marino S, Cilfone NA, JMattila JT, Linderman JJ, Kirschner DE. Dynamic balance of pro- and anti-inflammatory signals controls disease and limits pathology. Immunol Rev 2018; 285: 147–167

[43] Povo-Retana A, Landauro-Vera R, Fariñas M, Sánchez-García S, Alvarez-Lucena C, Marin S, Cascante M, Boscá L. Defining the metabolic signatures associated with human macrophage polarisation. Biochem Soc Trans 2023; 51: 1429–1436

[44] Espín JC, Larrosa M, García-Conesa MT, Tomás-Barberán F. Biological significance of urolithins, the gut microbial ellagic Acid-derived metabolites: the evidence so far. Evid Based Complement Alternat Med 2013; 2013: 1–15

[45] Piwowarski JP, Stanisławska I, Granica S, Stefańska J, Kiss AK. Phase II conjugates of urolithins isolated from human urine and potential role of β-glucuronidases in their disposition. Drug Metab Dispos 2017; 45: 657–665